

**VISUAL INSPECTION SYSTEM TO DETECT
CONNECTOR TILTS IN PCBAs**

by

VITHYACHARAN RETNASAMY

**Thesis submitted in fulfilment of the
requirements for the degree of
Master of Science**

January 2005

ACKNOWLEDGEMENTS

To every successful completion of work there will be a guiding beacon of light. I would like to express my profound gratitude and sincere thanks to my supervisor, Associate Professor Dr. Mani Maran Ratnam for sacrificing much of his precious time to provide me with constant guidance, advice and encouragement throughout the course of study. I will always be indebted for the support he has given.

I would also like to express my gratitude to my parents for their unconditional love, sacrifice and support throughout my program study. They have also been my pillars of strength during hard times of my course of study. A heartfelt thanks to Mr.Sathya Narayanan who have been constantly giving me encouragement and guidance throughout my life. I would also like to record my sincere thanks to my sisters, brother-in-law and little Dhurvasa for their unwavering moral support they have given.

My gratitude and appreciation to all the staff of the School of Mechanical Engineering, Univeriti Sains Malaysia, for their invaluable ideas and support. My special thanks to Mr. Hamid and Mr.Komaruddin for the support given.

My special thanks to Mr.R.Sivam for his guidance during my tenure in Solectron Technology, whom gave me the knowledge and experience needed in completion of my course of study. Lastly my sincere thanks to all my friends whom have given me great moral encouragements and spiced up my life during my duration spent here.

TABLE OF CONTENTS

	Page
ACKNOWLEDGMENTS	ii
TABLE OF CONTENTS	iii
LIST OF FIGURES	vii
LIST OF TABLES	xi
ABBREVIATIONS	xiii
LIST OF SYMBOLS	xv
ABSTRAK	xvii
ABSTRACT	xix
CHAPTER 1 INTRODUCTION	1
1.1 Research background	1
1.2 Research problem	3
1.3 Research objectives	6
1.4 Research scope	6
1.5 Research approach	7
1.6 Thesis organization	8
CHAPTER 2 LITERATURE REVIEW	10
2.1 Introduction	10
2.2 General automated visual inspection systems	10
2.3 3D Inspection on PCBA	13

	Page	
2.4	2D inspection on PCBA	15
2.5	3D inspection on other applications	22
2.6	Summary	25
CHAPTER 3	STUDY ON SEVERITY OF CAMERA LENS DISTORTION AND DETERMINATION OF SCALING FACTOR	26
3.1	Introduction	26
3.2	Camera height and zoom setting	27
3.3	Camera lens distortion severity analysis and scaling factor determination for different object heights	32
	3.3.1 Lens distortion theory	32
	3.3.2 Methodology	36
	3.3.3 Results and discussion	38
3.4	Summary	51
CHAPTER 4	ILLUMINATION ANGLE CALIBRATION OF NON-COLLIMATED LIGHT SOURCE	52
4.1	Introduction	52
4.2	Theory	53
	4.2.1 Application of the phase-shifting method	57
4.3	Illumination angle calibration on a single block surface	60

	Page
4.3.1 The method of least squares	65
4.4 The development of reference table	75
4.5 Verification of illumination angle calibration across the field of view	81
4.6 Summary	87
CHAPTER 5	88
TILT ANGLE MEASUREMENT ON	
CONNECTORS USING PHASE-SHIFT	
FRINGE PROJECTION	
5.1 Introduction	88
5.2 Methodology	89
5.2.1 Tilt measurements on glass blocks	89
5.2.2 Tilt measurements on connectors	92
5.3 Results and discussion	97
5.3.1 Glass block tilt measurement	97
5.3.2 Connector tilt measurement	109
5.3.2.1 Connector tilt measurement on artificial PCBA	109
5.3.2.2 Connector tilt measurement on actual PCBA	116
5.4 Summary	122
CHAPTER 6	123
SUMMARY AND FUTURE WORK	
6.1 Conclusions and project contribution	123
6.2 Future work	126

REFERENCES**128****APPENDICES**

Appendix A. Results for point distance measurement difference at different height levels

Appendix B. Results for rectangular sections absolute measurement differences at different height levels

Appendix C. Full data representation of partial data in the thesis

Appendix D. To Read Two Lines For Pixel Value Matching

Appendix E. To Read Two Lines, Match Pixel Value And Compute The Height Difference.

Publication List

LIST OF FIGURES

	Page
Figure 1.1: A few samples of PTH components, (a) e-caps, (b) power connector, (c) edge connector and (d) USB connector.	3
Figure 1.2: Soldering of connector leads.	4
Figure 1.3: (a) Tilt along the length of the PCI connector, (b) Tilt seen from a top view as in a direct overhead single camera AVI system.	5
Figure 3.1: Camera height setting from datum, with image (inset) sample used.	28
Figure 3.2: (a) Simulated image and line intensity plot, (b) real image from camera height 420 mm with line intensity plot, (c) real image at camera height 500 mm with line intensity plot and (d) real image at camera height 580 mm with line intensity plot.	30
Figure 3.3: Experimental setup of the research project.	31
Figure 3.4: Image showing part of grid with length measurement direction.	32
Figure 3.5: (a) Ideal lens condition, (b) barrel distortion and (c) pincushion distortion.	34
Figure 3.6: A barrel distorted image radial distance ρ pixel and an actual radial distance R mm.	34
Figure 3.7: Lens distortion severity graph.	35
Figure 3.8: Location of reference line on grid.	37
Figure 3.9: (a) Square grids before superimposing and (b) square grid after superimposing onto the reference grid.	38
Figure 3.10: Quarters and nodes to be measured on the square grid.	39
Figure 3.11: Different object height level.	39
Figure 3.12: Plots of ρ against R for object height (a) 0 mm, (b) 4 mm, (c) 8 mm, (d) 12 mm, (e) 16 mm and (f) 20 mm.	42

	Page
Figure 3.13: Designated points for verification of scaling factor.	44
Figure 3.14: Above are the sample block images printed on a paper.	47
Figure 3.15: Average scaling factor versus object height.	50
Figure 4.1: Collimated light source of the fringe projection illuminating the block surface.	54
Figure 4.2: Non-collimated light illuminating block surface.	56
Figure 4.3: A mirror mounted on a rotary stage.	58
Figure 4.4: (a) Solid blocks without fringes, (b) to (d) image of blocks with fringe projection: the fringes being shifted by 0, $2\pi/3$ and $4\pi/3$ respectively, (e) phase map produced from images (b)-(d).	59
Figure 4.5: (a) Block with fringe projection , (b) phase map of the block.	61
Figure 4.6: Laser measurement instrument for height verification.	62
Figure 4.7: Variation of θ with L mm before linear fitting.	65
Figure 4.8: Variation of θ with L mm after linear fitting.	69
Figure 4.9: Introduction of tilt on the block shows the shift of illumination angle from the horizontal surface to the tilted surface.	70
Figure 4.10: A saw-tooth line profile from a phase map image.	71
Figure 4.11: Tilted block height plots using different measurement methods.	74
Figure 4.12: Plots of θ versus L before linear-fitting for heights: (a) 2 mm, (b) 3.88 mm, (c) 5.73 mm, (d) 7.62 mm, (b) (e) 9.60 mm and (f) 11.57 mm.	77
Figure 4.13: Graph plots after linear-fitting for relationship between θ and L for heights: (a) 2mm, (b) 4mm, (c) 6mm, (d) 8mm, (e) 10mm and (f) 12mm.	79
Figure 4.14: Shows graph plot of both before and after linear fitting for, (a)–(b) block 1, (c)-(d) block 2, (e)-(f) block 3 and (g)-(h) block 4.	84

	Page
Figure 5.1: Blocks positioning and labeling.	90
Figure 5.2: The artificial PCBA made from glass sheet.	93
Figure 5.3: Connector surface edge where pixel reading was done using C++ program.	95
Figure 5.4: Actual PCBA with mounted Peripheral Component Interconnect (PCI) connectors.	96
Figure 5.5: (a) to (c) image of blocks with fringe projection: the fringes being shifted by 0 , $2\pi/3$ and $4\pi/3$ respectively, (d) phase map produced from images (a)-(c).	98
Figure 5.6: Height measurement plot along distance L mm on the tilted block surfaces for (a) block A, (b) block B and (c) block C.	99
Figure 5.7: Spots on phase map image causing spikes on height measurement data.	99
Figure 5.8: Height measurement plot along distance L mm on the tilted block surfaces for (a) block A, (b) block B and (c) block C after applying median filter on the phase map	100
Figure 5.9: Phase shifting and laser height measurement after linear fitting process for blocks: (a) block A, (b) block B and (c) block C.	103
Figure 5.10: Phase map of blocks using the second set spacer thickness.	105
Figure 5.11: Phase shifting and laser height measurement after linear fitting process for blocks: (a) block A, (b) block B and (c) block C.	107
Figure 5.12: (a) to (c) image of connectors with fringe projection: the fringes being shifted by 0 , $2\pi/3$ and $4\pi/3$ respectively, (c) phase map produced from images (a)-(c).	111
Figure 5.13: Height measurement data along connector length L mm on the tilted connectors surface edges (a) connector A, (b) connector B and (c) connector C.	112
Figure 5.14: Phase shifting and laser height measurement after linear fitting for connectors: (a) A, (b) B and (c) C.	114

Figure 5.15: Five connectors investigated and labeled.	117
Figure 5.16: (a) to (c) image of blocks with fringe projection, the fringes being shifted by 0, $2\pi/3$ and $4\pi/3$ respectively.	119
Figure 5.17: Phase map of the connectors on an actual PCBA	120
Figure 5.18: Height measurement data using phase shifting technique is linear fitted for, (a) connector B, (b) connector C, (c) connector D and (d) connector E.	121

LIST OF TABLES

	Page
Table 3.1: Average scaling factor values for different quarters.	40
Table 3.2: Average S values.	44
Table 3.3: Result for level 0mm.	45
Table 3.4: Result for level 20 mm.	48
Table 4.1: Partial data for coordinate and grayscale value along lines in the background and the block.	62
Table 4.2: Pixel value match along two lines.	63
Table 4.3: Calculation of θ value.	64
Table 4.4: Partial data used in obtaining the best-fit line.	68
Table 4.5: Data obtained after the linear fitting.	68
Table 4.6: Measured points on the tilted block using laser instrument.	72
Table 4.7: (a) Data for block height after linear fitting process using phase-shifting technique and (b) block height data after linear fitting process using laser measurement instrument.	73
Table 4.8: Height measured for stacked glass pieces using laser instrument.	76
Table 4.9: Reference table.	80
Table 4.10: Partial data of solid glass block 1.	82
Table 4.11: (a) Data of block 1, (b) Data of block 2, (c) Data of block 3 and (d) Data of block 4 after linear-fitting.	83
Table 4.12: Difference analysis of height measurement between laser instrument and phase-shifting method.	86
Table 5.1: Tilt angle comparison between laser and phase-shifting computation for first set spacer thickness.	101
Table 5.2: Tilt angle comparison between laser and phase-shifting computation for second set spacer thickness	106

Table 5.3: Tilt angle comparison between laser and phase-shifting computation for connectors.

ABBREVIATIONS

AOI	Automated Optical Inspection
AVI	Automated Visual Inspection
BGA	Ball Grid Array
CAD	Computer Aided Design
CCD	Charged Couple Device
DFP	Digital Fringe Projection
DIP	Dual In-Package
FOV	Field of View
IC	Integrated Circuit
LED	Light Emitting Diodes
MIL	Matrox Imaging Library
PCBA	Printed Circuit Board Assembly
PCI	Peripheral Component Interconnect
PGA	Pin Grid Array
PPM	Part Per Million
PTH	PinThrough Hole
PWB	Printed Wire Board
ROI	Region of Interest
SMD	Surface Mount Devices
SMT	Surface Mount Technology
SOT	Small Outline Transistors
THM	Through Hole Mount
USB	Universal Serial Bus

2D	Two Dimension
3D	Three Dimension

List Of Symbols

- A - Uniform background Intensity
- B - Amplitude of sinusoidal light
- G - Gray scale intensity distribution
- I - Intensity
- L - Length in millimeter
- H -Horizontal distance in millimeter
- R - Radial distance in millimeter
- S - Average scaling factor
- SD - Standard deviation
- SSE - residual sum of squares due to error
- V - Vertical distance in millimeter
- h - Horizontal distance in pixel
- r - Radial distance in pixel
- v - Vertical distance in pixel
- y - Object height
- \bar{L} - Mean value for distance
- r_1 - Undistorted image radius
- S_h - Horizontal scaling factor
- S_r - Radial scaling factor
- S_v - Vertical scaling factor
- S_{LL} - Sum of squared deviation of L
- $S_{\theta\theta}$ - Sum of squared deviation of θ
- $S_{\theta L}$ - Sum of product L deviation with θ

- S^2 - Variance
- e'_i - Residual between observed and predicted value
- δx - Distance in fringe shift
- θ - Projection angle
- θ' - Predicted value of θ
- $\bar{\theta}$ - Mean value of θ
- ρ - Radius distorted image
- β, α - Coefficients of radial distortion
- $\phi(i,j)$ - Phase angle at (i,j)
- β_0 - Interception on θ' axis
- β_1 - Slope of best fit line

Sistem Pemeriksaan Visual untuk Mengesan Kecondongan Penyambung di dalam PCBA

ABSTRAK

Sistem pemeriksaan visual automatic memainkan peranan penting dalam bahagian tapisan kualiti di industri eletronik. Kebanyakan system viaual ini mempunyai hanya satu kamera overhed yang tidak dapat memreriksa kecondongan penyambung di dalam PCBA. Disertasi ini mempersembahkan pembangunan sistem pemeriksaan visual satu kamera untuk mengesan kecondongan komponen penyambung di dalam PCBA. Sistem ini dibangunkan dengan menggunakan komputer peribadi, kamera digital, projector slaid dan cermin. Kadar kecacatan di dalam sistem imej dikaji dahulu untuk memastikan sama ada sistem camera perlu dikalibrasi atau tidak. Masalah dan objectif penyelidikan ini adalah untuk membangunkan sistem pemeriksaan visual satu kamera untuk mengesan kecondongan komponen penyambung di dalam PCBA dengan bantuan teknik anjakan fasa. Suatu persamaan untuk menentukan faktor julat pada ketinggian permukaan objek yang berlainan dihasilkan secara eksperimen. Faktor skala ini digunakan untuk menukarkan koordinat piksel imej kepada ukuran metrik milimeter. Projector slaid digunakan untuk memancarkan pinggir di atas permukaan yang dikaji.. Cermin yang dipasang pada bahagian pemutar digunakan untuk proses anjakan fasa. Cahaya yang digunakan didalam penyinaran ialah tak selari alur cahayanya. Sudut alur tuju cahaya ini berubah didalam arah x -, y - dan z -. Kalibrasi dilakukan untuk menghasilkan persamaan untuk arah tuju cahaya tak selari dengan jarak pada arah x - pada atas permukaan objek yang dikaji untuk ketinggian yang berlainan. Blok kaca

digunakan pada awal eksperimen untuk menguji dan mengesahkan system ini. Kaedah anjakan fasa digunakan untuk mengira sudut kecondongan pada blok kaca dan penyambung. Sistem visual ini yang berasaskan keadah teknik anjakan fasa berjaya mendemonstrasikan untuk mengesan dan mengira ketinggian kecondongan pada penyambung yang dipasang di PCBA. Sistem ini berbanding dengan yang sedia ada ialah ia menggunakan satu kamera overhead, cahaya tuju yang tak selari alurnya dan kaedah anjakkkan fasa untuk mengesan kocondongan penyambung di dalam PCBA.

Visual Inspection System to Detect Connector Tilts in PCBAs

ABSTRACT

AVI's are playing important roles in quality inspection in the electronic industry. Most existing AVIs are single overhead camera and are incapable detecting 3D defects. This thesis presents the development of a single camera visual system to detect tilt of a Peripheral Component Interconnect (PCI) connector on a Printed Circuit Board Assembly (PCBA). The visual system developed consists of a personal computer, digital camera, slide projector and a mirror. The problem in the current research and the objective is to detect tilt in a PCI connector using a single overhead camera. The distortion severity in the imaging system was initially studied to decide the need for camera calibration. An equation was formulated experimentally to determine the scaling factors at different height levels of object surface for converting image pixel coordinates into physical dimension. The slide projector was used for projecting sinusoidal fringes onto the surface under study. Phase-shifting was achieved using a mirror mounted on rotary stage. Since the light source used is non-collimated, i.e. the incident angle varies along x-, y- and z- directions, a calibration exercise was carried out to obtain an equation for the incident angle of the beam along the length of the object surface for different object height levels. Solid glass blocks were initially used in place of actual PCI connectors to test and verify the system. The phase-shifting technique was applied to calculate the tilt angles on the glass blocks and later applied to the actual connectors. This visual system developed using phase-shifting technique demonstrates successful tilt detection and measurement in a PCBA. Compared

to existing system the proposed system uses single overhead camera , non-collimated light source and phase shifting technique to detect tilt on a connector mounted to a PCBA.

CHAPTER 1

INTRODUCTION

1.1 Research background

Inspection has long been an integral part of quality control in many industries ranging from agricultural to the high-end electronic industry. The process of determining if a product deviates from a given set of specification is defined as inspection (Newman and Jain, 1995). Inspection involves measurement of specific part features such as surface finish and geometric dimensions (Newman and Jain, 1995). Human inspectors have been predominantly carrying out the visual inspection tasks in most industries. However requirements of the modern manufacturing environment have intensified the usage of automated visual inspection (AVI) systems (also known as automated optical inspection (AOI) system). The main requirement of modern manufacturing demand for the emergence of machine vision systems is the trend towards total quality, that is products with zero defects (Moganti and Ercal, 1996).

AVI systems are playing major roles in the semiconductor, container, wood, food, automobile and other industries (Rao, 1996), (Newman and Jain, 1995). In the electronic sector, machine vision system is currently gaining prominence in the Surface Mount Technology (SMT) industry where various products using printed circuit board assembly (PCBA), ranging from small mobile phone circuit boards to the high-end telecommunication and server

circuit boards, are manufactured. Total quality trend coupled with PCBA evolution into high complexity of board sizes and various mixture of components is slowly pushing human inspectors towards the edge of elimination. A research done by Teradyne concludes that human inspectors can only detect 50% of visible PCBA board defects (John, 2000). The repetitive and demanding nature of inspection makes concentration hard to maintain. Furthermore, human inspectors are prone to visual fatigue. AVI systems on the other hand have high consistency, repeatability and are not affected by fatigue factors. Considering the trend of PCBA evolution and human inspection factors, AVI systems seems to be the solution for visual inspection tasks.

An AVI systems cost can vary from as low as USD30,000 up to USD200,000 or more (Newman and Jain, 1995). Companies from Machine Vision Technology Ltd, Orbotech, Omron and Teradyne have AVI systems ranging from solder paste inspection till full PCBA boards. Currently there are no available AVI systems for the inspection of every single component in a PCBA for high-mix low volume and high-mix high volume circuit boards (Sakie, 2001). This situation creates the need for human inspection. Components that cannot be inspected by the AVI system need to be inspected by human inspectors. The hurdles obstructing the AVI systems to be used in 100% fully automated inspection mode are tasks where such systems lack decision making and inspection flexibility (Rao, 1996), (Newman and Jain, 1995). The decision making tasks arises when an observation falls into the border of acceptance and failure criteria definition. Human intervention is required in this stage. An AVI system with a single overhead camera has flexibility limitations

for inspecting certain defects. Defects such as tilted or lifted pin through hole components (PTH, or sometime known as THM – through hole mount components) pose limitation for such single camera systems. This research focuses on developing a single camera visual system for inspecting the PTH connector tilt defect.

1.2 Research problem

PTH components are mostly inspected by human operators. The types of components in this category include e-caps, edge-connectors, Universal Serial Bus (USB) ports and connectors as shown in Figure 1.1. PTH components are placed manually by human operators and are soldered in the protruded leads below the PCBA. This is done by a molten solder in a wave machine as shown in Figure 1.2.

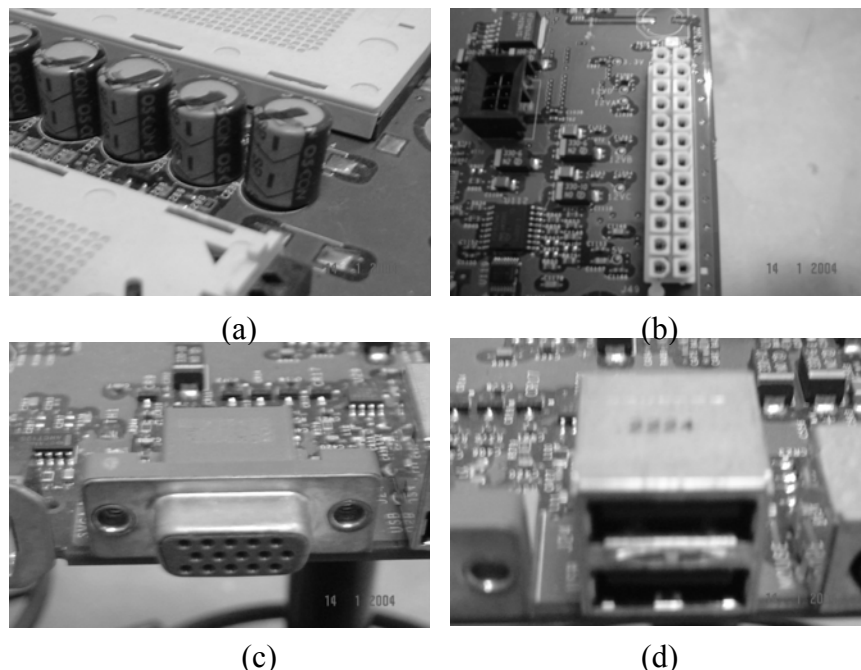


Figure 1.1: A few samples of PTH components, (a) e-caps, (b) power connector, (c) edge connector and (d) USB connector.

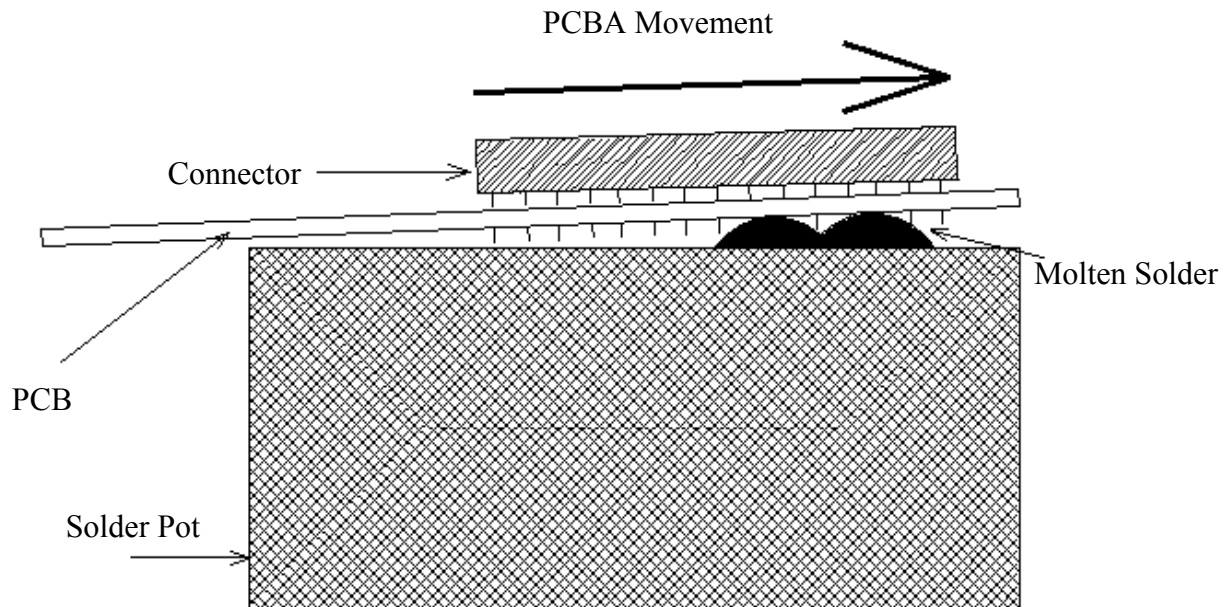


Figure 1.2: Soldering of connector leads.

Either during manual assembly or wave soldering process, defects in PTH components occur. According to a study by Yeow and Sen (1999), tilt of components is a one of the major problem in the manual assembly area. Components that are easily tilted are usually loose fit. These components are jerked while traveling on the wave soldering machine conveyor. Other factors are due to environment conditions that induce the operators to insert the components wrongly. Their study also showed that manual assembly components have a high customer defect return and tilt is a major concern. A study done by Oresjo (2000) shows that the defect level for the PTH joints are rather high, i.e. as much as 3,976 part-per-million (ppm). The average defect level is at around 1100 ppm. Twenty percent of the PTH joint defects arise from missing pin defect. Missing pin is mainly due to either tilt of the component or a

pin of the connector is pushed in improperly. This, however, rarely occurs as most connectors are loose fit. Figure 1.3 shows various views of a Peripheral Component Interconnect (PCI) connector tilt.

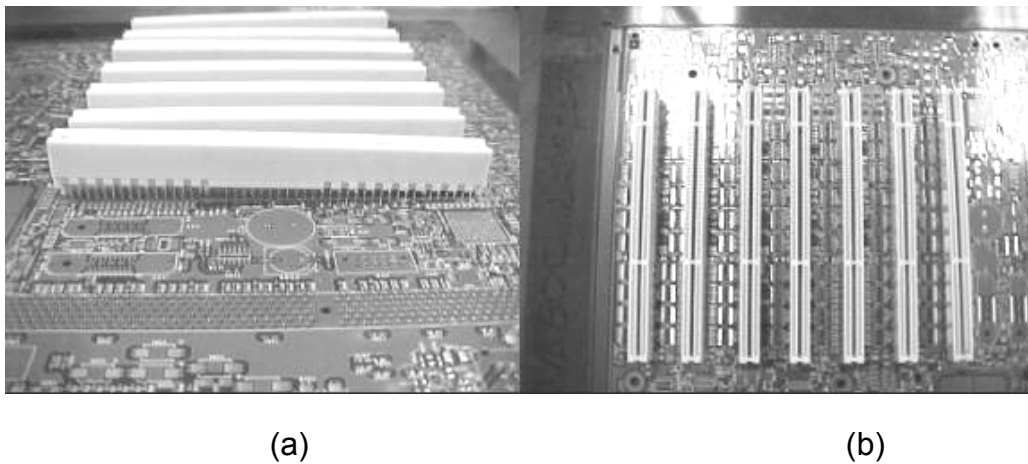


Figure 1.3: (a) Tilt along the length of the PCI connector, (b) Tilt seen from a top view as in a direct overhead single camera AVI system.

The tilt defect in Figure 1.3(a) can be still detected using the current state of the art multiple view camera but such a system is costly for an example Orbotech, Trion series with 13 CCD cameras. The problem in the current research is to detect tilt in a (PCI) using a single overhead camera.

1.3 Research objectives

The main objective of this project is to develop a single camera visual system to detect tilt of a PCI (as in Figure 1.3) on the PCBA board. In this visual system an overhead digital camera was used to capture the two dimensional (2D) images by using a non-collimated light source. In order to achieve the main objective the sub-objectives as detailed below was addressed:

- i) Camera lens distortion severity was studied.
- ii) Non-collimated light behaviour was investigated and applied for measurement.
- iii) Phase-shifting technique was applied to measure the tilt height on both the connectors and glass blocks.

1.4 Research scope

The scope of this research covers the subject of camera lens distortion study, scaling factor generation, the behaviour of non-collimated light for measurement and using of phase-shifting technique for height calculation. The research was done accordingly as:

- i) Square grids were used to investigate the lens distortion severity.
- ii) Data obtained in the lens distortion study was also used to formulate an equation to convert pixel coordinates of image into physical dimension in millimetre.
- iii) Phase-shifting method was applied to measure the tilt height, which would be later converted into tilt angle.
- iv) Non-collimated light was used to measure tilt heights, the illumination angle was derived from a reference table.

- v) The data in the reference table need to be interpolated to get illumination angle for a given height within 11.57mm.
- vi) Tilt angle was calculated from the height measured, this was demonstrated on both glass blocks and connectors placed on a flat surface.
- vii) Finally the tilt angle measurement was demonstrated on an actual PCBA.

1.5 Research approach

Three main approaches were used to study and solve this research problem. A study on the distortion severity in the imaging system for the digital camera was also carried out. Since conversion of pixel coordinates of image into physical dimension in millimetre needs a scaling factor for different object heights, an equation to determine the scaling factors for different object height has been derived experimentally. A slide projector was used for the structured lighting projection. The light source of the projector is a non-collimated beam. The varying incident angle of the non-collimated ray was calibrated before conducting the experiments. Glass blocks were used initially for the experiment. Glass blocks have no top surface grooves and holes as on a connector. Phase-shifting technique was used to calculate the tilt angles of the blocks. Finally phase-shifting technique was implemented on actual connectors to calculate tilt angles.

1.6 Thesis organization

The thesis is divided out into six chapters. Chapter 1 (Introduction) gives a brief review on the background of the research. The research problem is identified in this section.

Chapter 2 explores previous literature on related works carried out by other researchers. The focus is on research carried out on three dimensional (3D) automated PCBA inspection. Importance is given on work related to 3D inspection of related studies. Previous researches done on PCB inspection are also reviewed.

Chapter 3 presents the work on digital camera lens distortion and calibration. Research on related area is briefly reviewed. This chapter also focuses on work done to formulate an equation for scaling factor calculation. The scaling factor was used to convert pixel coordinates to physical dimension in millimetre. The equation enables scaling factor computation for different height levels from the datum.

In Chapter 4, a study on calibration was done on non-collimated light source used for projecting structured lighting. This light source has varying angle of illumination in the field of view (FOV). The illumination angle calibration was carried out, and the effectiveness of the calibration was tested at different locations in the FOV. An equation was derived for the angle of illumination at different object heights.

In Chapter 5, tilt angle calculation was conducted on four multiple glass blocks. Height measurement were also done using laser instrument to verify the accuracy of the phase-shifting technique. The final section was on tilt angle calculation for the actual connectors mounted on a specially designed PCBA. This calculation was also carried out on the actual PCBA board of mounted components.

Finally Chapter 6 concludes the thesis by summarising the research contributions and suggestion for future work.

CHAPTER 2

LITERATURE REVIEW

2.1 Introduction

This chapter reviews past work done on automated inspection of printed circuit board assembly (PCBA), particularly work done on 3D inspection of PCBA. Areas of research done on 2D inspection of PCBA were also briefly reviewed. Finally 3D inspections on other application are reviewed.

2.2 General automated visual inspection system

The surface mount technology (SMT) in the world is undergoing dramatic changes (Downing and Owen 2000). These changes have made impacts on SMT companies such as:

- Addition of new production line, which are moved, modified and upgraded at a faster rate.
- Integration of expectations, standards and quality procedures.
- Flooding of high-technology products and new component types entering the factory.

With the trend of total quality, miniaturization of components, highly complex circuitry and variety sizes and shapes of components makes the functionality of human inspectors inefficient. (Downing and Owen 2000) Automated visual inspection (AVI) systems seem to be the only supplement to cater for these requirements, with its untiring eyes.

Rao (1996), gave a comprehensive review on the future direction of the industrial machine vision. 3D surface analysis and classification is the next phase growth of the AVI systems in the electronics industry. The drive behind this growth comes from two sources, the availability of better sensor and the increasing complexity of the manufacturing process itself. Inspection that requires 3D information uses techniques such as sensor input of binary, gray scale and colour images are not practical. Rao added that this trend in decreasing geometries applies to all area of computer manufacturing, this implies that inspection systems must use higher sensitivity sensors and resolution. As a conclusion it can be said that integration of information from multiple cue, such as colour, height and texture is becoming significant for many applications.

Newman and Jain (1995) have done a survey on automated visual inspection systems and techniques. A presentation of taxonomy based on sensory input of the AVI systems is discussed here. A total of five sensory based inputs are reviewed which are:

- Inspection using binary images
- Inspection using grey level images
- Inspection using range images
- Inspection using others sensing modalities

Binary based systems have good advantages considering the hardware and software requirements are at minimum. However, they are not adequate for many inspections of surface characteristics and 3D shapes. Vision systems that use grey level intensity have low capability in performing inspection in complex

industry environment of dirt and unfavourable lighting condition. These systems use image subtraction or localized histogramming methods for defect detection. Electronics industry provides favourable condition for this input. Colour inspection task are very appropriate for AVI systems regardless of the industry using it. Impediments such as high computing power, intricate optics and controlled lighting makes colour AVI systems deployment less popular. Inspection using range images have been used to extract 3D information. To name a few methods used in this range images are structured lighting, stereo camera technique and moiré interference pattern. This range images is discussed in detail at Section 2.5. Inspection using other sensing modalities, are like x-ray, ultra-sound, gamma rays and infrared sensing. These applications are highly customized for certain defect inspection only.

Newman and Jain (1995) have also given a detailed insight on AVI technique approaches. Two general approaches in defect detection in AVI techniques are defined. The first is template matching and second is feature extraction of sensed image. A defect free image will be used as a template for matching a sensed image object. If the sensed object matches well than the object is defect free. Feature extraction of sensed object is based on certain list of description and rule. If all the rules are satisfied, than the sensed object is defect free. The computer aided design (CAD) inspection was given extra importance by Newman and Jain. This CAD based design was used as a inspection template. CAD template based inspection systems are much desired in selected industries because the models contain exact specification of an object. The CAD database can also be embedded with information such as

material type, geometric tolerances, desired surface quality finish and finish colour which would provide unified description applicable for inspection systems. The CAD models inspection system has a great disadvantage when the inspected object has a short shelf life span. Products which have dimension features changing rapidly will have great setback in inspection term if CAD based models are used. This is because image forming of models in CAD is highly complex and time consuming. In short CAD based inspection models are not flexible to cater the fast product evolution.

2.3 3D inspection on PCBA

Work done by Guerra and Villalobos (2001) is the closest to the subject of this research. The objective of their work is to develop a 3D inspection system for surface mount devices (SMD) assembly that are reliable and inexpensive. The inspection operation presented in their paper consists of detecting the presence and absence of components. The components inspected here are chip resistors, chip capacitors, small outline transistors (SOT) and capacitors. This system utilizes sheet-of-light triangulation technique, whereby the board is illuminated with laser. The geometric properties of the system are utilized to calculate the height values for each reflection of the sheet-of-light. This paper defines four inspection algorithms, which are, (a) LUTMETH, (b) HISTMETH, (c) AVGMETH and (d) MEDMETH, whereby METH refers to method and LUT is look up table, HIST is histogram, AVG is average and finally MED is medium. All methods manipulated the threshold values to develop the algorithms in detecting the presence and absence of the SMD components. All methods have an average inspection time of 216 seconds to

inspect 484 components of a TV motherboard. The advantage of this system is factors such as lighting conditions and component colour variation does not affect the inspection. The disadvantage is the time factor, a typical 2D vision system takes approximately 30 seconds to inspect the same PCBA completely and not just the selected components. The system is not practical in the current surface mount technology (SMT) industry, due to the high volume of boards produced. An existing 2D vision system may cater the need for fast detection of the absence and presence of the components described above.

The other papers dealing with 3D inspection of PCBAs, which are remotely related, are work carried out by Kelley et al. (1988) and Svetkoff and Doss (1987). Both the papers describe work done on single spot laser beam triangulation technique to obtain range values. The major drawback with this method is only one range value per frame can be obtained at one time. This will consume a lot of time to inspect even selected components on a typical computer motherboard.

In summary, there are no published works related to 3D connector inspection of printed circuit board assembly (PCBA). Papers available of work done on 3D inspection of PCBAs are as reviewed. This shows clearly that there is still a need to develop 3D inspection systems for variety of components in the SMT industry.

2.4 2D inspection on PCBA

There are a number of papers published on 2D inspection of PCBAs mainly focusing on SMD component defects. To the best of the author's knowledge there are no papers even on 2D inspection of connectors and other pin through hole (PTH) component defects. Generally the papers reviewed in this section focus defect inspection on SMD components and solder joints.

Teoh et al. (1990) developed technique to inspect five different types of SMT defects, namely, missing components, misaligned, wrong orientation of integrated circuit (IC) chips, wrong parts and poor solder joints. The technique used in detecting missing, misaligned and wrong orientation component is the pixel frequency summation. This concept involves two steps, which are, (1) obtaining a histogram distribution graph (pixel frequency vs grey level values) and (2) summing the pixel frequencies over a chosen range of grey values. In detecting the missing component, a window is defined anywhere within an IC component. The pixel value frequency distribution is calculated within this window. The frequency of the pixel value was different for IC present and missing. The same concept on missing component is used for detecting the misaligned chip, but here the window defined encloses the entire chip. If there is a misaligned frequency of pixel value, than the distribution has difference. Every dual in-package (DIP) chip component has a white strip on its surface. This white strip was used to detect the wrong orientation of this component. A window defined will enclose this white strip, in the situation of wrong orientation the white strip was missing, so the frequency of pixel value distribution is different for both the cases of white strip absent and present. To detect wrong

IC part, the concept of Run-Length Encoding was employed in this paper. A window was used to enclose the IC characters on the surface. These characters were used to differentiate this IC chip from a wrong part. Solder joint inspection was done by inspecting the normalized volume and standard deviation of the solder joints. The inspection of solder bridges was done by checking the area between the solder joints for white pixels. In summary the defects discussed in this paper covers the general commonly seen defects on SMD component. The wrong IC part detection is applicable if only the characters are printed in white. Generally only ball grid array (BGA) components have character printed in white, for ICs the character printing is done on dark beige coloured characters. These characters will not have the distinct difference of black and white to use the Run-Length Encoding. The windowing concept for misaligned will trigger false calls for components with surface of same colour depth of the PCB surface. The distribution of the pixel value frequency will not be clearly distinct. Misaligned of such components will not be an easy detection using the method stated.

Kishimoto et al. (1990) developed a PCBA inspection system that uses colour image processing with multi-lighting technique. This system uses three types of lighting to perform inspections. These lightings were switched on according to the type of inspection and the type of part inspected. Firstly, the colour lighting was used for inspecting missing and incorrectly positioned parts. The second lighting method used is the vertical lighting used in inspecting solder joints. The last method is the oblique lighting used for inspecting solder bridging. The concept of projecting slit lighting is for an object mounted the slit

image is observed broken and shifted when viewed from an angle. If the component is missing, than slit image is continuous without breaks. Using this phenomenon inspection for parts missing and incorrectly positioned were carried out by detecting the edges of the slit image. The slit lighting has a problem when, parts having a specific height of integral multiple of 5 mm. The adjacent slit light will overlap with the one on the part. The edges were not detected in such cases, even the part was not missing. In such cases a coloured light source in the sequence of red, blue and white were projected. This was than evaluated through colour image processing. Parts of edges not detected even by using coloured lighting, due to overlapping slit lights, were than solved by using the galvano mirror to change the projection angle. Inspection to detect the solder presence is done by using the vertical lighting projected at the same angle as that of the camera on to the solder. The principle here is, if the solder is formed correctly, the surface will reflect light in a direction different from that of the camera. The will result in low brightness. In the case of missing solder, light reflected from the board surface (the solder pad) will have high brightness. Light was projected in a different angle (called oblique lighting) from that of the camera view was used in inspecting solder bridge. In this case high brightness is due to the presence of solder bridge. In this work, components due to missing because of knock-off incident is defined as not missing using the slit lighting. A knock-off component is due to bad handling of PCBA board, where by the component will have part of the body being knocked off. In this case slit lighting projected will form a break and edge would be detected. With the trend of miniaturization, slit lighting projected has to be of fine lines with optimum angle of projection. Slit lighting would be a major

drawback for components positioned in between connector and for components of dark colour.

Yohko (1989), developed a four angled camera vision system to detect defects such as solder bridging and missing components. This system is based on a 2Dimensional vision. The use of angled cameras enables the system to acquire views with perspective without using 3Dimensional vision techniques. Combining the images from different cameras, a solder joint can be examined in multiple directions, hence getting a result similar to that of human inspection. The inspection of defects, use brightness, grey level and binarization methods. This system developed in this paper has made no whatsoever reference to the speed of inspection in the PCBA. The accuracy of defect detection is at around 99.9% and 99.5% for the defects stated previously. Inspection speed is an important factor in this fast paced, high volume SMT industry.

David and Cihan (1997), have discussed the advantages of implementing an intelligent visual inspection system based on natural human vision. The development of intelligent sensing and decision making system is essential in performing a task traditionally executed by human beings. The discussion in this paper is focused in developing an artificial neural network, similar to the vision and perception derived from human aspect. The examples given here are like detecting edge automatically, understanding a image which has incomplete features and focusing on region of interest (ROI) naturally without processing the entire image to determine the ROI. This enhanced vision system will increase the efficiency of the automated visual inspection process.

The intelligent models will allow current vision systems to possess additional human characteristics, such as perception and attention. With this every aspect of an image would not be considered. Attention was quickly focused on misplaced and misaligned part or a defect that appears uncharacteristic. Their paper did not show the results and testing done on actual shop floor of the manufacturing industry. A system described such as above would be the ideal vision system in a SMT industry, but validation on real situation is much needed to prove the capability of the system.

David and Sai-Kit (1988), have developed a tiered colour illumination approach for machine inspection of solder joints. A tiered lighting arrangement is used to generate colour contours on the solder joint for the detection and classification of defects including no solder, insufficient or excess solder, poor wetting of component leads or solder pad and faults due to improper insertion of component leads. This paper focuses on solder joint of pin through hole (PTH) component leads. A low angle red light is positioned 5 mm above the PCBA, which illuminates the solder fillet. A high angle blue light is placed 150 mm above the PCBA, which illuminates the solder pad. For a good solder joint with uniform concave shaped filled, the result image of the joint would contain a small red ring bounded by a blue ring when viewed directly above the joint. Using the thresholds selected for each of the red and blue image planes, the x-coordinates of transitions along each horizontal scan line are recorded (Run-Length Code). Geometric features of closed contours are calculated from traversal of the vertex points and accumulation of the following quantities, (1) area, (2) perimeter, (c) circularity and (d) centroid coordinates. Combination of

these measurements for each red and blue contour and any associated hole contours can be used to produce variety of classification features. The advantage of the tiered illumination system is that flaw detection and classification is based on simple geometric features in separate colour planes of the image. This method has been successfully tested on samples of commercially manufactured, wave soldered circuit boards. The capability and efficiency of this method has yet to be tested on a real manufacturing condition. The speed of inspection is not specified here, which was a major factor for deploying to the shop floor of manufacturing.

Kim et al. (1999) have developed a technique using multi layered lighting system to detect and classify solder joint defects of SMD components. Three layers of ring shaped light emitting diodes (LED) with different illumination angles were used and three frames of images were obtained in sequence. From this images, the ROI (soldered regions) are segmented, and their characteristic features including the average grey level and the percentage of highlights referred to as 2D features are extracted. Based on the back propagation algorithm of neural networks each solder joint is classified into one of the pre-defined defect types. This solder joint was classified based on the Bayes classifier. In short, in this paper the defect classification use two stage classifier approach. In conclusion the system described in the paper shows good experimental results on sample solder joint tested. Full 3D feature extraction shows longer time, a combination of both 2D and 3D gives the best optimum output. Performance of this system on real time situation has yet to be known.

Kashitani et al. (1993) developed a prototype system for inspection of solder joints between printed wired boards (PWB) and surface mounted pin grid arrays (PGA). This system illuminates the solder joints using an optical fibre light guide and acquired its images using a charged coupled device (CCD) sensor that was connected to an optical fibre image guide. This system extracted possible defect locations in the images using fuzzy clustering. The system was tested on images of 7100 good solder joints and four bad solder joints. The system was able to detect all bad solder joints and nearly all good solder joints. This system has a false alarm rate of less than 1%.

Hara et al. (1988) used a technique based on subtraction of a registered input image from an image of an ideal sample printed wiring board (PWB, term used earlier to printed circuit board). The input image was aligned with the reference image using alignment marks. This system was illuminated with ultraviolet light and detected fluorescence emitted by boards base material. This emitted light was filtered optically with band pass filter to produce a two colour image. Several image processing operation were used to allow line features to be reliably inspected. The authors have tested this system on images of boards containing artificial defects.

Park and Tou (1991) developed a system that inspects for common PWB component defects. This system collects images from three viewpoints. A dual channel processing paradigm was followed to process these component images. The system correctly classified over 77% of the component inspected.

2.5 3D inspection on other applications

Quan et al. (1999) used an on-contact optical method based on fringe projection technique for 3D shape measurement of a hydroformed shell. In this work the sinusoidal fringes were produced by the interference of two spherical wavefronts from the output fibre. The fringe patterns were captured by a camera and gratings were using the camera negatives. A slide projector was used in this work to project the fringe patterns onto a hydroformed shell. Though deformed fringe pattern image is acquired by a CCD camera and Fourier transform is performed on the image using a microcomputer. This work in conclusion describes a method for obtaining three-dimensional surface contouring. The major drawback of this method is the accuracy of measurement, which is lower, compared with the phase-shifting method.

Huang et al. (1999) have developed a digital fringe projection (DFP) technique for detection and quantitative evaluation of corrosion on engineering structures. The DFP detects and evaluates corrosion by measuring surface topographical changes caused by corrosion. This technique uses digital projection display technology, which provides the capability of digitally projecting fringe patterns with extremely high brightness and contrast ratio. Specially developed software is used to create the fringe patterns, which allows instant changes of intensity profile, phase and spacing. Phase wrapping and unwrapping are done automatically by specially developed software. A high resolution CCD camera was used to measure a total of 4 million surface contour data were generated for each measured specimen. The advantage of the

described technique is it does not need any moving parts and provides 3D contours of corrosion specimens instantly.

Hsueh and Antonsson (1997) have done work on developing a fast, high-resolution, automatic, non-contact 3D surface geometry measuring system using a photogrammetric optoelectronic technique based on lateral-photo effect diode detectors. This system has been designed for acquisition of surface geometries such as machined surfaces, biological surfaces and deformed parts. The system can be also used in design, manufacturing and inspection and range finding. A laser beam is focused and scanned onto the surface of the object measured. Two cameras in stereo positions capture the reflected light from the surface at 10 kHz. Photogrammetric triangulation will transform the pair of 2D signals created by the camera detectors into 3D coordinates of the light spot. This system can only illuminated a small spot at one time. In the manufacturing industry where time is the essence, this needs to be improved further.

Robotic Vision Systems developed a structured light sensor and MC-68000 based image processing system to acquire 3D data. (Schmidt, 1984) The sensor has been used for inspecting large propeller surfaces (propellers are up to 24 ft in diameter) for the United States Navy. The same system was also used for inspecting engine castings for Cummins Engine, where 1250 dimensional inspection were required. (Schmidt, 1984) Sheet metal hole, edge features and weld seams on production line at General Motors, Westinghouse

and Caterpillar also used the same system, which uses the structured light sensor. (Lee,1990)

Pryor (1982) developed several inspection systems using structured lighting. The systems reviewed in brief are:

- 1) A system that inspected the eccentricity in the line of contact between gear teeth and tooth spacing errors in gears at a rate of one pair of mating gears every 10 seconds.
- 2) Another system qualified and sorted bolts on 10 different dimensions at rates of 10,000 bolts per hour.
- 3) A third system inspected the internal bores of a power steering housing, performing complete inspection for surface defects such as pits, scratch, voids, tool marks and crack in less than six seconds.
- 4) The next system used twelve cameras to inspect the dimension of engine valves at a rate of 4200 valve inspection per hour on a production line.
- 5) Power steering worm assemblies were inspected at a rate of 1500 parts per hour using two cameras and two microcomputers.
- 6) Threaded and machined hole in cylinder heads were inspected using 80 image sensors to check the presence of thread in every hole and to detect hole blockage.

The listed inspection systems above were used with high accuracy in extracting 3D information for defect inspection.